Astronomical and Astrophysical Transactions (*AApTr*), 2019, Vol. 31, Issue 3, pp. 251–266,
ISSN 1055-6796, Photocopying permitted by license only, ©Cambridge Scientific Publishers

Dynamics of solar microwave emission before powerful flares in September 2017

I.A. Bakunina[1,*], V.F. Melnikov[2]

[1] *National Research University Higher School of Economics, Nizhny Novgorod, Russia*
[2] *Pulkovo Observatory (Russian Academy of Sciences), Saint-Petersburg, Russia*

Received 1 October, 2018

In this paper, we describe the spatial structure and time characteristics of the microwave emission of active region AR 12673 during the rapid changes in the magnetic flux from September 3 to September 6, 2017 using Nobeyama Radioheliograph observations. It is shown that the microwave emission of the active region exhibits extremely non-stationary behavior of both spatial brightness distribution and total flux, even at the time of no pronounced soft X-ray flare activity. We also found significant oscillations of the Stokes parameters I and V with characteristic times of 1.5 hours or less.

Keywords: Sun: active regions: flares: microwave emission

1 Introduction

It is known that flare activity on the Sun is associated with the emergence of an essentially new magnetic flux in active regions (AR) (Künzel 1960; Severny 1960, 1988; Ishkov 1998). In recent years it was concluded that the most characteristic sign of the preparation of a large flare is the formation of the structure of magnetic field like "SHIL" type (Strong-field, High-gradient polarity Inversion Line) (Schrijver 2016; Harra et al. 2016; Toriumi et al. 2017).

The active region 12673, which produced the most powerful flares of the 24th solar activity cycle from September 4 to 10, 2017, is a vivid example of a demonstration and complex, delta-configuration, magnetic field, and rapid changes in the magnetic flux. It has already been studied in sufficient detail for the evolution and features of the magnetic flux behavior under observations with high spatial resolution of the HMI (Helioseismic and Magnetic Imager) magnetometer on board the space observatory SDO (Solar Dynamics Observatory) (Hou et al. 2018; Sun & Norton 2017; Yan et al. 2018; Wang et al. 2018). These papers report on very rapid emergence of a new

*Email: rinbak@mail.ru

magnetic flux in AR 12673, starting from the 3rd of September. In this case, the counter-clockwise rotation of the main sunspots of the group and also the formation of shearing motion between the sunspots and the S-shaped structure were observed. In addition, the existence of a flux rope between the main sunspots is found before the onset of each flare. The strong shearing motion and rotation contributed to the destabilization of magnetic flux ropes, which, most likely, was the cause of powerful flares in AR 12673.

Microwave radiation is a very sensitive indicator of the changes in the parameters of an active region (the concentration of nonthermal electrons, the temperature and density of plasma, the strength and spatial structure of the magnetic field). Therefore, the use of its observable characteristics to diagnose the processes occurring before flares and coronal mass ejections (CME) is very promising. The purpose of this paper is to check out how the above mentioned changes in magnetic field of active region 12673 influence the spatial structure and time characteristics of the microwave emission of this active region during the period from September 3 to September 6, 2017.

2 Observations and data analysis

In September 2017, active region NOAA 12673 evolved from a crumbling sunspot of the northern magnetic polarity to the most active AR of the 24th cycle of the solar activity. It produced 52 X-ray flares C, M and X class from the 4th to the 10th of September, including 4 flares above X1.0 GOES class (including X9.3, September 6, 2017 and X8.2 on 10 September), and also 8 flares above M3 class. Its high flare activity is associated with the emergence of a new magnetic flux. The ascent of the magnetic flux began on September 3 to the southeast of the old sunspot (the remainder from ARs 12665 and 12670) (Fig. 1) and continued until the AR entered the limb edge on September 10th.

Our analysis has been performed on the basis of solar radio maps obtained with the Nobeyama Radioheliograph (NoRH) at the frequency of 17 GHz with a two-dimensional spatial resolution of 10″–15″, cadence interval between images of 10 s and integration time of 10 s. We were interested in spatial and temporal dynamics of the microwave emission at the beginning of the magnetic flux surfacing on September

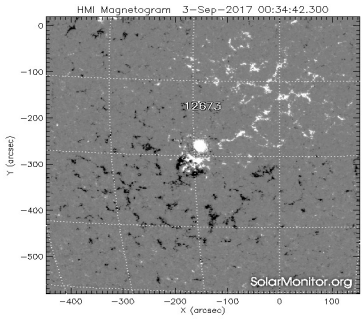


Figure 1 Magnetic field distribution on the photosphere level on September 3, 2017 obtained from SDO/HMI magnetograms.

3, when the active region did not produce X-ray bursts, as well as in the interval of several hours before the X-ray flare of class M1.2 (September 4, 2017), before four flares on September 5, 2017 of M3.2 (04:33), M1.0 (03:42), M4.2 (01:03), C9.8 (00:30) classes and before the flares of C2.7 (07:29), X2.2 (08:57), X9.3 (11:53) classes, which occurred beyond the interval of observations of the Nobeyama Radioheliograph (from 22:50 to 06:20 UT) on September 6.

3 Microwave emission on September 3, 2017

The spatial structure of the radio source at frequency 17 GHz on this day is shown on Fig. 2 (left panels) for two moments of time, at the beginning of the NoRH observation

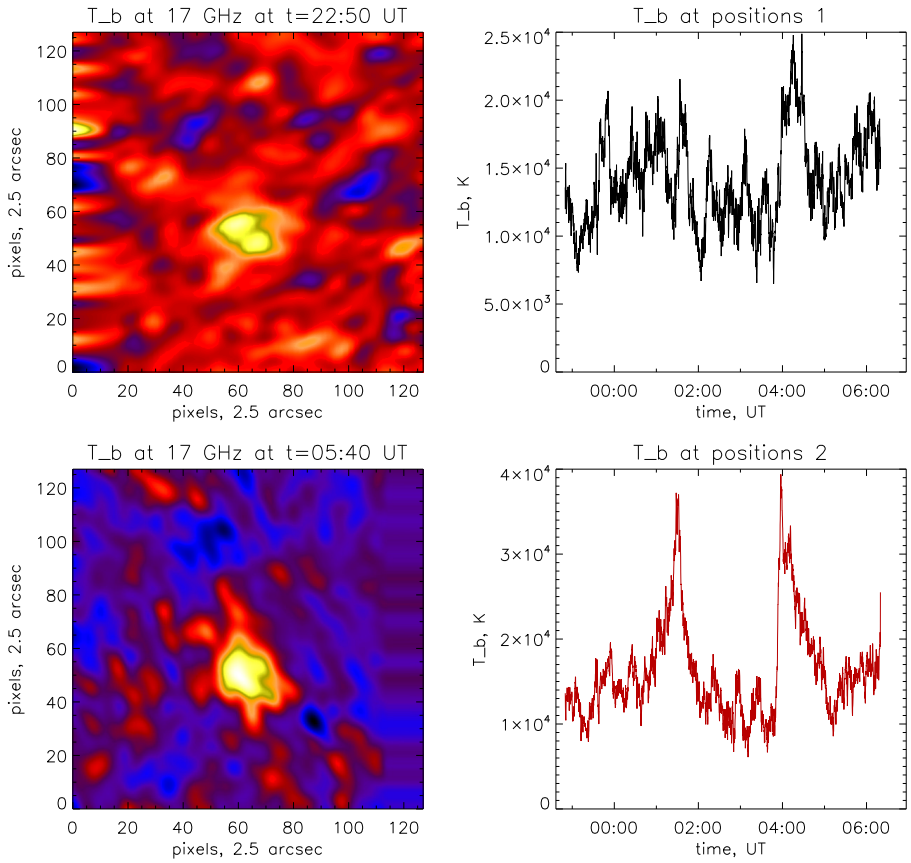


Figure 2 Spatial structure of the microwave source and brightness temperature time profiles at 17 GHz on September 3, 2017. Upper panel: on the left – 17 GHz brightness distribution at time 22:50 UT / 2017-09-02; on the right – time profiles of brightness temperature at 17 GHz from position 1 [66,49], the integration time of the signal is 50 s. Bottom panel: on the left – 17 GHz brightness distribution at 05:40 UT / 2017-09-03; on the right – time profiles of brightness temperature at 17 GHz from position 2 [63,56], the integration time of the signal is 50 s.

period, and at its end. Temporal behavior of the radio brightness temperature from the two centers of brightness is shown on the right panels. We can see that the radio source is rather weak, its brightness temperature hardly exceeds 3×10^4 K. Radio emission is almost non-polarized during observations on that day. However, one can note a significant non-stationarity in intensity (Fig. 2) and total flux (Fig. 3), as well as some complication of the spatial structure of the radio source at the end of the NoRH observations on September 3, 2017. Oscillations with periods of 6 min, 15–30 min in the intensity and Stokes V parameters as well as in total flux are well seen on Figs 2 and 3. The long lasting and relatively weak radio bursts were observed over the newly formed region of a complex magnetic structure (S–N–S) (Fig. 1; Fig. 2, lower panel). Presumably, this is the area of the emerging new magnetic flux.

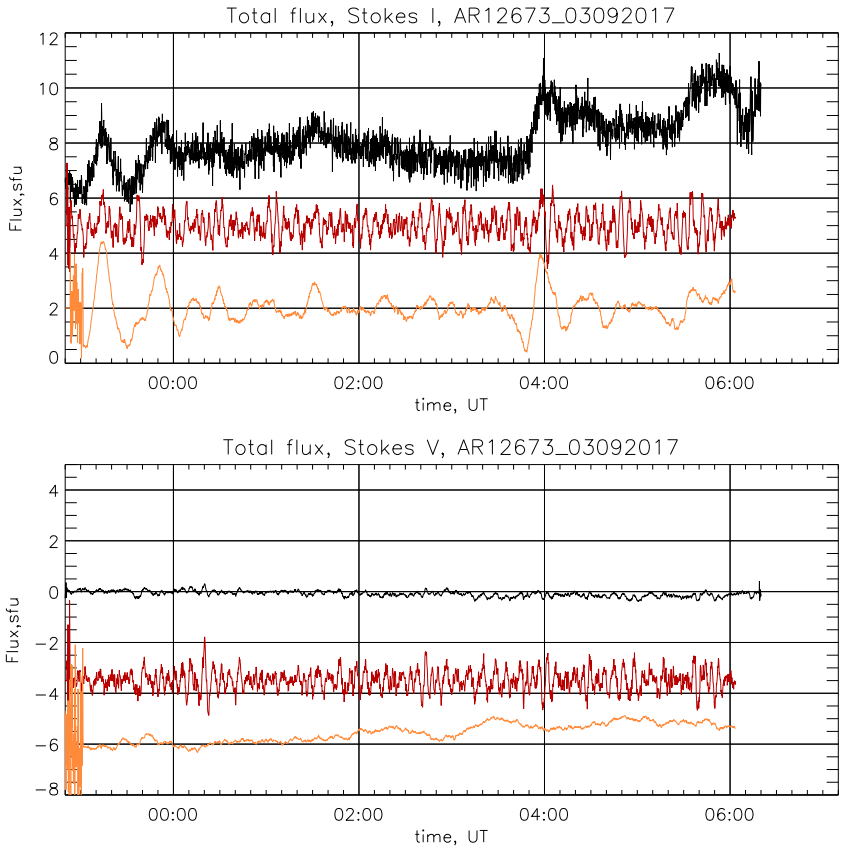


Figure 3 Time profiles of the microwave emission of active region on September 3, 2017: the total flux in intensity (upper panel), polarization (lower panel). In the top panel, black color curve shows total flux; red color -curve is the high-frequency component obtained by subtracting from the total flux its values smoothed over tau = 400 c, multiplication factor k = 5; orange color curve is the high-frequency component obtained by subtracting the signal component smoothed over tau = 1400 c from the smoothed over tau = 400 c, multiplication factor $k = 3$. In the bottom panel, black color curve shows the full flux of Stokes parameter V, the red and orange are high-frequency components obtained in the same way as for the top panel but with the multiplication factors $k = 6$ and $k = 6$, respectively.

4 Microwave emission on September 4, 2017

The new magnetic structure, which began to form on September 3, became more complex and expanded on September 4. The old sunspot of the northern polarity (in the center on the magnetogram, Fig. 4) was surrounded by a complex quadrupole structure of the magnetic field.

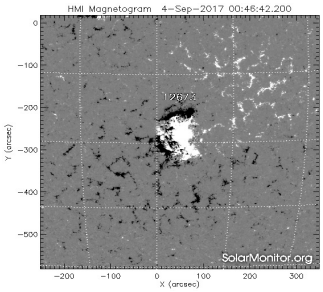


Figure 4 Magnetogram of SDO/HMI on September 4, 2017.

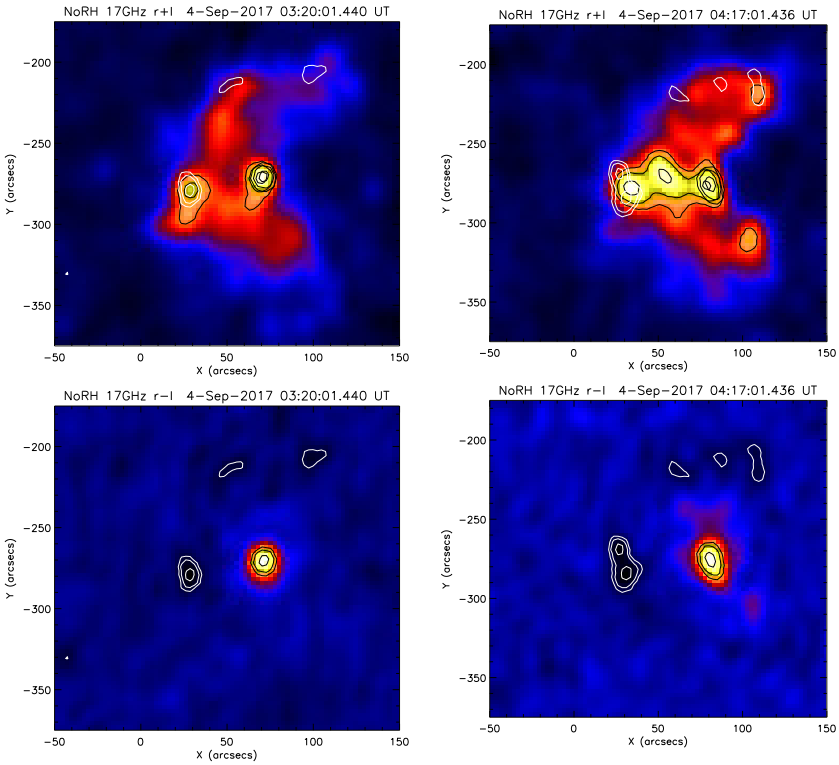


Figure 5 Structure of the radio source in intensity (Stokes parameter I) (upper image) and in polarization (Stokes parameter V) (bottom image) at two moments of time, 03:20 UT and 04:17 UT, on September 4, 2017. The black contours correspond to positive polarization, the white – negative.

On September 4 the spatial distribution of radio brightness changes radically. At the beginning of observation (22:50 UT) it consists of two almost parallel loop-like structures elongated in the direction "north–south" with the positive polarization of the southern foot and negative polarization of the northern foot (Fig. 6, left panel). About 2.5 hours before the M1.2 class X-ray flare ($t_{st} \approx$ 05:36 UT), the spatial structure completely changed: a bright loop-like structure elongated in the direction "east–west" appeared. In Fig. 5, one can see the appearance of negative polarization to the east of the old positively polarized sunspot. Later on, this "horizontal" structure continues to increase its brightness and becomes the main source of the powerful microwave emission of the M 1.2 class X-ray flare (see Fig. 5 and the lower left image on Fig. 6). Note that this new horizontal microwave structure connects the old magnetic field of the northern polarity with the newly emerged magnetic flux of southern polarity.

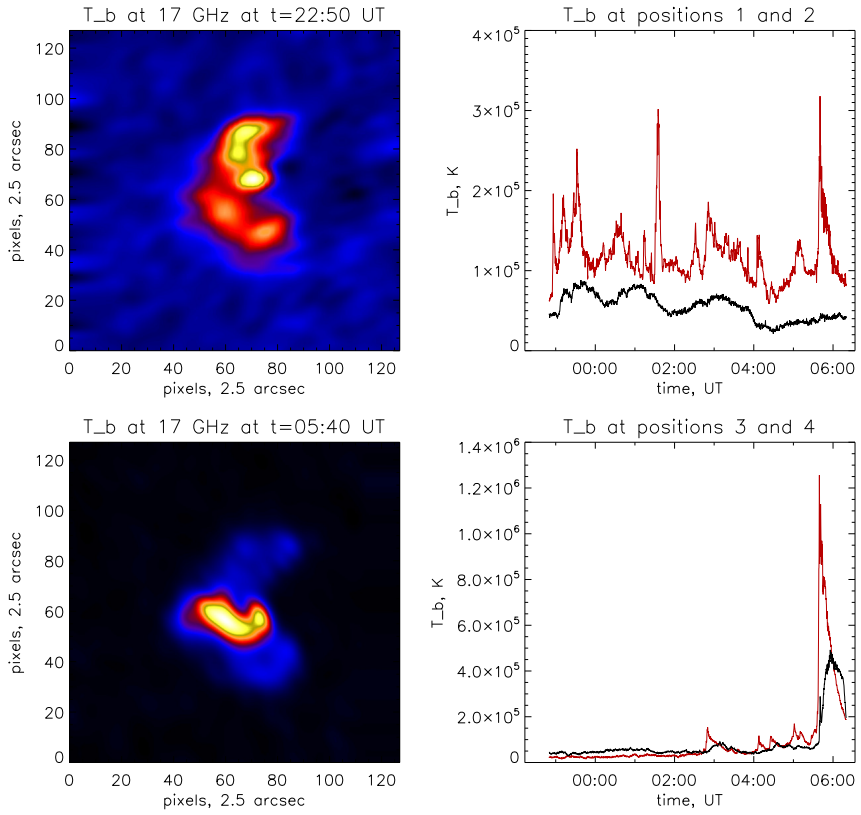


Figure 6 Structure of the radio source at 17 GHz and the brightness temperature temporal profiles from specific positions on September 4, 2017. Top panel: on the left – 17 GHz brightness distribution at time 22:50 UT / 2017-09-03; on the right – time profiles of brightness temperature at 17 GHz from positions 1 – [66,83], black line and 2 – [71,66], red line; the integration time of the signal is 30 s. The bottom panel: on the left – the distribution of brightness at 17 GHz at 05:40 UT / 2017-09-04; right – time profiles of brightness temperature at 17 GHz from positions 3 – [60,55], black line and 4 – [73,57], red line, integration time of signal – 30 s.

The right panel of Fig. 6 displays temporal changes in the brightness temperature from different areas of the radio source. The southern part of the "north–south" loop-like structure (with its center's coordinates [66,83]) demonstrates relatively regular smooth and weak ($\Delta T < 5 \times 10^4$ K) oscillations with the periodicity of about 2 hours. Unlike this, the above mentioned "east–west", or horizontal, structure shows very strong brightness temperature variations: ($\Delta T > 2 \times 10^5$ K) with characteristic times from $\tilde{1}0$ min to $\tilde{1}.5$ hours from the position with coordinates [71,66]. One can see that the region of maximum microwave brightness is the region with coordinates [73, 57], which is closer to the western edge of the horizontal structure. Note that the powerful flares on September 5 happened in the close vicinity of this structure.

In Fig. 7, we show time profiles of integrated (with no spatial resolution) Stokes I and V parameters in interval within 6.5 hours before the beginning of the first

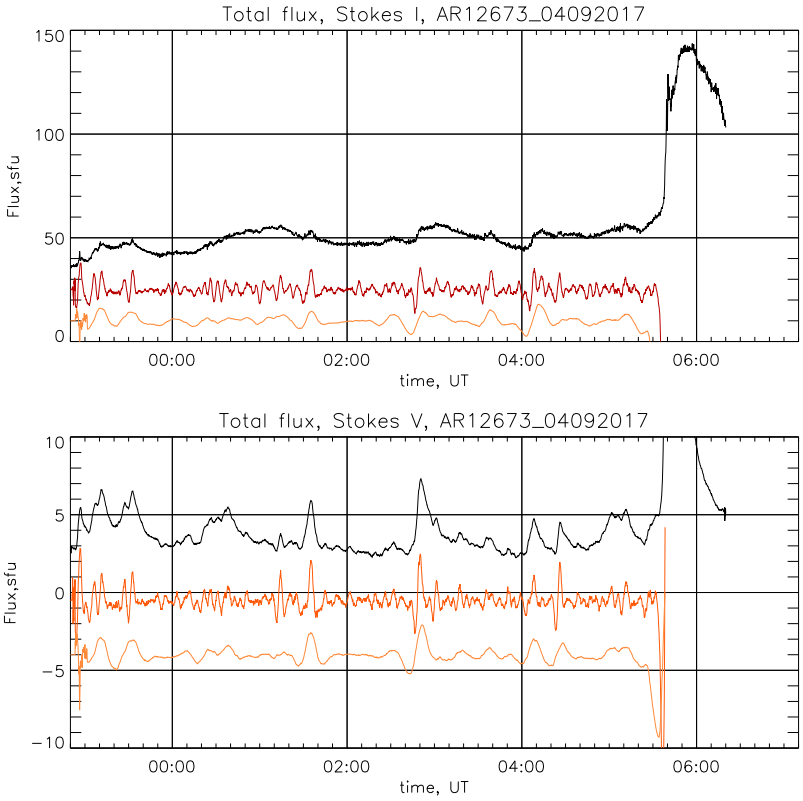


Figure 7 Time profiles of the microwave emission of active region on September 4, 2017: the total flux in intensity (upper panel), polarization (lower panel). In the top panel, black color curve shows total flux; red color curve is the high-frequency component obtained by subtracting from the total flux its values smoothed over tau = 400 c, multiplication factor k = 10; orange color curve is the high-frequency component obtained by subtracting the signal component smoothed over tau = 1400 c from the smoothed over tau = 400 c, multiplication factor $k = 3$. In the bottom panel, black color curve shows the full flux of Stokes parameter V, the red and orange are high-frequency components obtained in the same way as for the top panel but with the multiplication factors $k = 3$ and $k = 1$, respectively.

powerful flare M 1.2 (05:36) in AR 12673. As one can see, the most pronounced peculiarity of these time profiles is the presence of quasi-periodicities with periods of about 6 min, 20 min, and 100 min.

5 Microwave dynamics on September 5, 2017

On September 5, the new magnetic structure continued to become more and more complicated. The magnetogram (Fig. 8) shows an increase in the magnetic flux of the southern polarity to the north from the old sunspot and the introduction of a new magnetic flux of southern polarity into the middle part of the AR (region of the old sunspot).

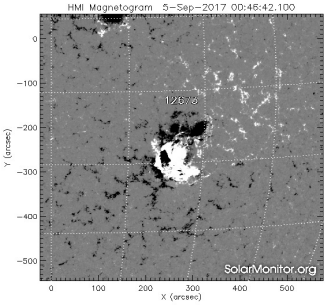


Figure 8 Magnetogram of HMI (SDO) on September 5, 2017.

Figure 9 illustrates the brightness distribution in the radio source on September 5. Again we see that the most intensive and variable place in the source is located in the vicinity of the mentioned earlier bright horizontal structure. For example, at positions with coordinates [55,63] and [56,59], variations of brightness temperature during 6.5 hours of observations reach more than 2×10^6 K. Sometimes the intensity enhancements are so impulsive that they may be classified as flares. Actually these enhancements are coincident in time with the X-ray flares observed on this day: C9.8 (00:30), M4.2 (01:03), M1.0 (03:42), M3.2 (04:33).

Time profiles of the total flux in intensity and polarization of the microwave emission from the whole active region are shown on Fig. 10. Similar to the day of September 4, we can see pulsations of different time scales, from 6–10 min to 100 min. Here, however, the quasi-periodicities are not so regular as on September 4.

6 Observations on September 6, 2017

On this day, the first most powerful flares X2.2 (08:57) and X9.3 (11:53) occurred in AR 12673 and during the 24th cycle of solar activity. On the magnetogram (Fig. 11), a greater increase in the magnetic flux of the southern polarity to the north of the old sunspot is noticeable and one can see its complication (the interspersion of the flux of the northern polarity). The image in the extreme ultraviolet from SDO/AIA, 193 A (Fig. 12) allows us to see the arcade structure above this area, and a very complex system of arches above the area of the old sunspot and to the south of it.

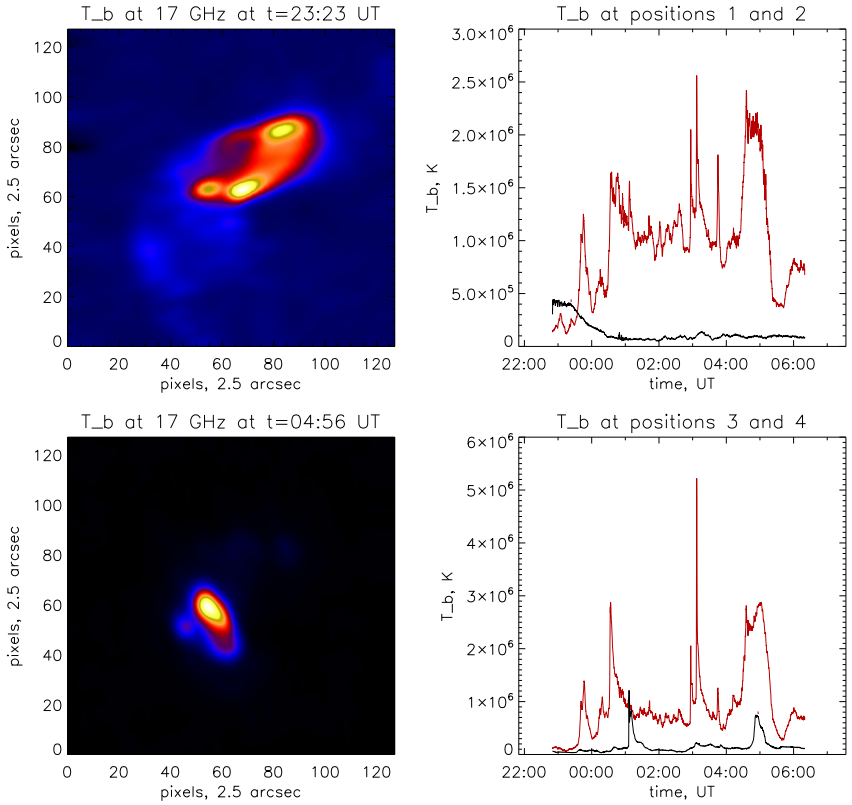


Figure 9 Structure of the radio source at 17 GHz and the brightness temperature temporal profiles from specific positions on September 5, 2017. Top panel: on the left – 17 GHz brightness distribution at time 23:23 UT/2017-09-05; on the right – time profiles of brightness temperature at 17 GHz from positions 1 – [68,63], black line, and 2 – [55,63], red line; the integration time of the signal is 30 s. The bottom panel: on the left – the distribution of brightness at 17 GHz at 04:56 UT/2017-09-05; right – time profiles of brightness temperature at 17 GHz from positions 3 – [47,51], black line and 4 – [56,59], red line, integration time of signal is 30 s.

According to Hou et al. (2018), on September 6, the rapid shearing motion along the PIL and rotation of the sunspot in the AR core region resulted in the kink-instability of a flux rope. Then this kink-unstable flux rope erupted upward and led to the successive eruptions of another two flux rope proxies within 5 min before the peak of the X9.3 flare. The evolution of the AR magnetic fields shows that five dipoles emerged successively at the east of the main sunspot. Probably significant flux emergence and successive cross-separations between the patches of different newly-emerging dipoles resulted in the formation of the omplex system with multiple flux rope proxies and the storage of huge magnetic energy.

During the NoRH observation interval (22:50–06:20 UT), no X-ray flares occurred. All important flares (C2.7 (07:29), X2.2 (08:57), X9.3 (11:53)) happened after this interval. Our analysis of the spatial dynamics of brightness in the intensity and polarization channels at 17 GHz shows that the spatial structure of the microwave source

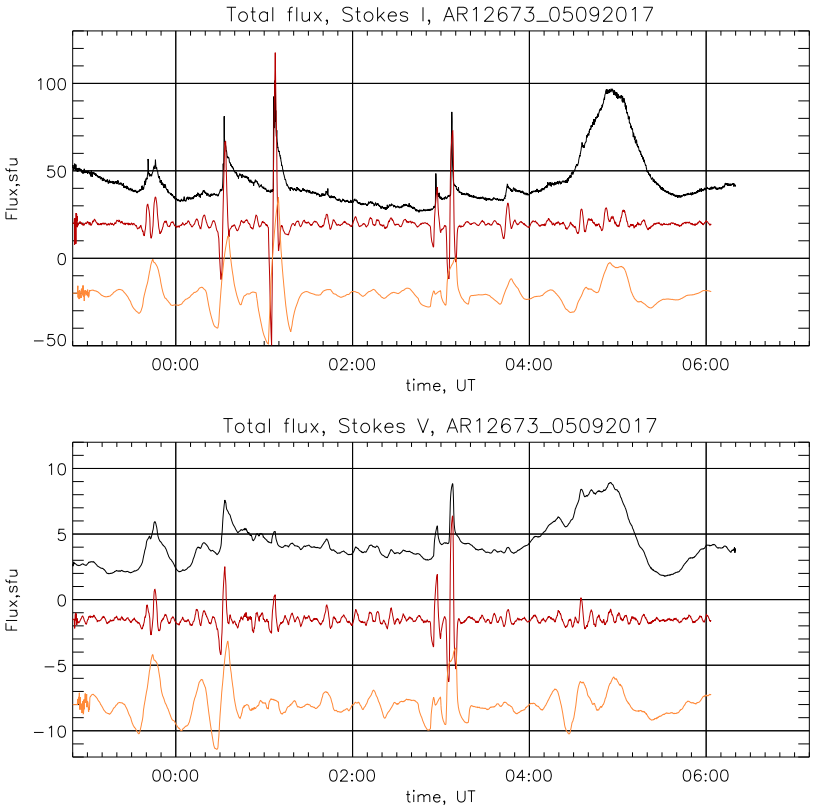


Figure 10 Time profiles of the microwave emission of active region on September 5, 2017: the total flux in intensity (upper panel), polarization (lower panel). In the top panel, black color curve shows total flux; red color curve is the high-frequency component obtained by subtracting from the total flux its values smoothed over tau = 400 c, multiplication factor k = 5; orange color curve is the high-frequency component obtained by subtracting the signal component smoothed over tau = 1400 c from the smoothed over tau = 400 c, multiplication factor $k = 3$. In the bottom panel, black color curve shows the full flux of Stokes parameter V, the red and orange are high-frequency components obtained in the same way as for the top panel but with the multiplication factor $k = 3$.

in intensity channel is quite stable. However, it changes dramatically in polarization, both in the western and eastern parts of the radio source (Fig. 13). At some moments, the three-core structure of the western part of the polarization map appears. Sometimes certain regions even change the sign to the opposite. This, most likely, indicates complex dynamics of the magnetic field a few hours before the first powerful flare. The magnetogram (Fig. 11) confirms this showing the appearance of a magnetic field of the southern polarity to the west of the old (northern polarity) field.

Integrated over the whole active region the time profiles of the microwave emission on September 6, 2017 are shown on Fig. 14. A comparison of these time profiles with ones for 3rd, 4th, and 5th of September shows many similarities, especially in the non-stationarity. However, we can see some specific differences. First of all, the average

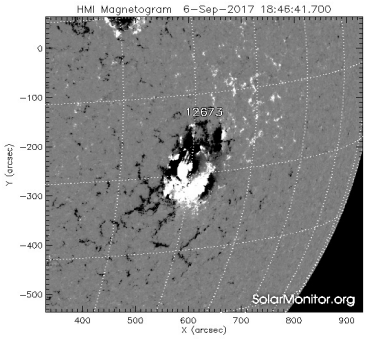


Figure 11 Magnetogram of HMI (SDO) on September 6, 2017.

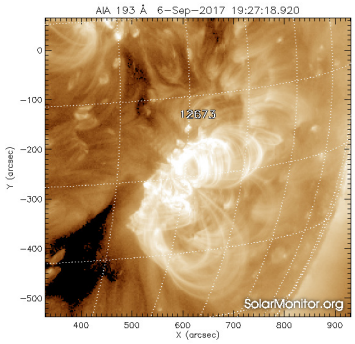


Figure 12 Extreme ultraviolet image at line 193 A from SDO/AIA on September 6, 2017.

brightness temperature grows significantly (by 2 orders of magnitude) day by day (compare Figs 2, 6, 9, 13). The same is also true for the total flux. Its average value increases from about 10 sfu on September 3rd, 2017 to about 50 sfu on September 4th and 5th, and to about 100 sfu on September 6th. Second, we can see much regular periodicities of 6, 20, and 100 min both in Stocks I and Stokes V total fluxes.

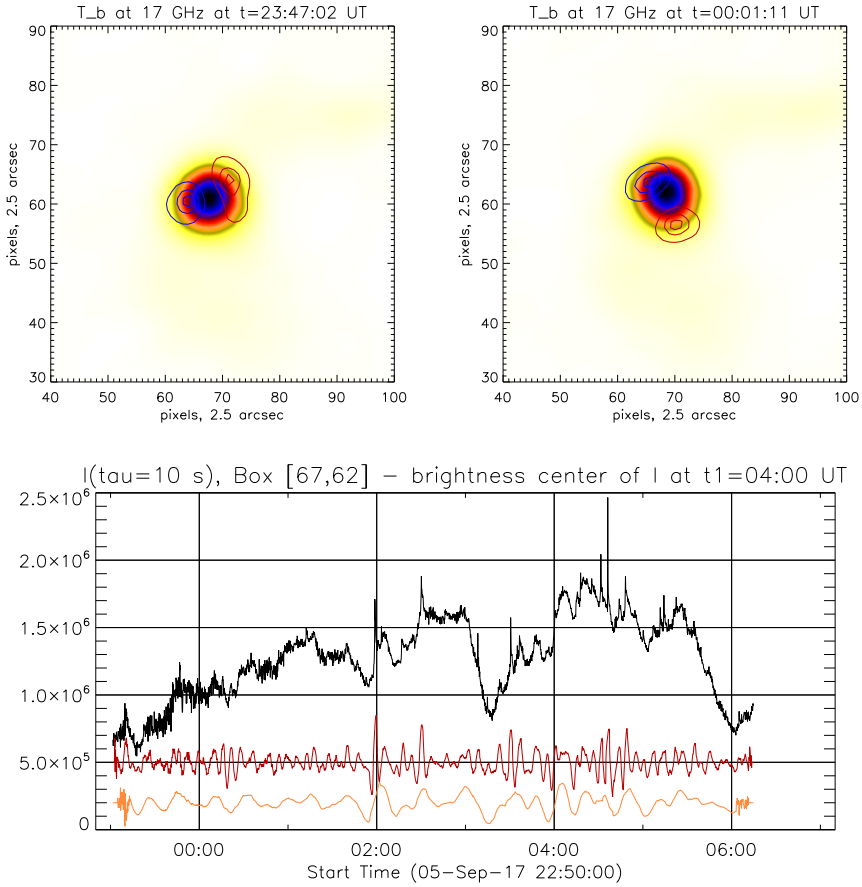


Figure 13 Radio brightness distribution over AR 12673 at 17 GHz on September 6, 2017. Upper plots: images in intensity (Stokes I) for two moments of time with overlayed contours of polarization intensity (Stokes V), red color – positive ($V = R - L > 0$), blue color – negative. Lower panel: Brightness temperature time profiles from the center part of the source [67,62]. Black color curve shows total flux; red color curve is the high-frequency component obtained by subtracting from the total flux its values smoothed over tau = 400 c, multiplication factor $k = 3$; orange color curve is the high-frequency component obtained by subtracting the signal component smoothed over tau = 1400 c from the smoothed over tau = 400 c, $k = 1$.

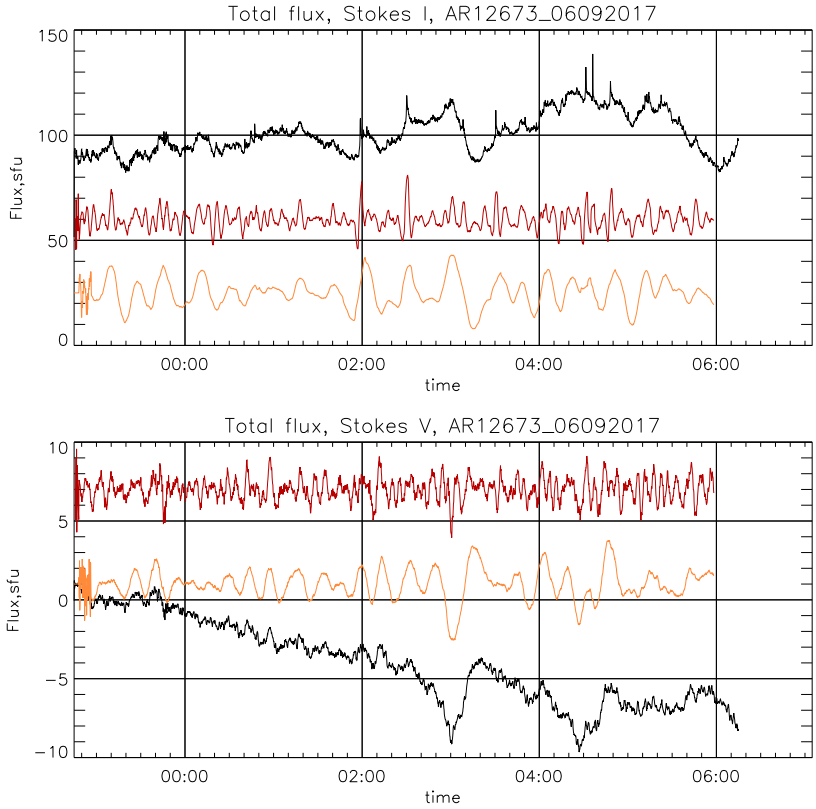


Figure 14 Time profiles of the microwave emission of active region on September 6, 2017: the total flux in intensity (upper panel) and polarization (lower panel). In the top panel, black color curve shows total flux; red color curve is the high-frequency component obtained by subtracting from the total flux its values smoothed over tau = 400 c, multiplication factor $k = 5$; orange color curve is the high-frequency component obtained by subtracting the signal component smoothed over tau = 1400 c from the smoothed over tau = 400 c, multiplication factor $k = 3$. In the bottom panel, black color curve shows the full flux of Stokes parameter V, the red and orange are high-frequency components obtained in the same way as done for the top panel.

Conclusions

In this study we consider the structure and dynamics of microwave emission in AR 12673 in the intensity and polarization for several days, namely for the period from September 3 to September 6, 2017 during the period of complex changes in the magnetic flux, before the flare of X9.3 class (11:53, September 6), the most powerful flare in the 24th cycle of solar activity.

1. It is revealed that the spatial structure of microwave sources before all the flares from September 4 to September 6, 2017 was remarkably unstable. The most changes happened to the spatial distribution of Stokes V polarization parameter.

2. Most of the time, the brightness temperature maximum was located in the central parts of bright loop-like structures of the active region, in the middle between opposite polarization maxima at 17 GHz.

3. Time profiles of the Stokes parameters I and V showed significant non-stationarity with characteristic times of about 100 min to 6 min. The average brightness temperature and total flux of microwave emission was growing day by day up to 100 and 10 times, respectively, from 3rd to 6th of September 2017.

4. The microwave brightness distribution in the active region 12673, as well as its whole microwave energetics changed radically on September 4th. On this day, the microwave source structure changed from the two almost parallel loop-like structures elongated in the direction "north–south" to the bright loop-like structure extended in the direction of "east–west". This horizontal structure continued to brighten not only on this day, but also on the next two days of observations, up to the end of September 6, after which the flare of X9.3 class (11:53) occurred.

5. The fluxes of total intensity and polarization underwent quasi-periodical oscillations with periods from 6 to 20–30 min, modulated by slower changes with characteristic time of 60–100 min.

We believe that the most likely reasons for such a spatial redistribution of radio brightness and temporal variations of microwave emission intensity are: a) reorganization of the spatial structure of the magnetic field of the active region before flares; b) activation of other (orthogonal) magnetic tubes with possible acceleration of electrons in them.

Acknowledgements

This work was supported by grants of RFBR Nos. 17-52-80064, 18-02-00856 and Program CAS 2016VWA044. The work was partly carried out with the Solar Data Analysis System operated by the Astronomy Data Center of the National Astronomical Observatory of Japan.

References

Künzel H., 1960, Astronom. Nachr. 285, 271
Severny A.B., 1960, Izv. KrAO, 22, 12

Severny A.B., 1988, Some Problems of the Physics of the Sun, M.: Nauka, 221 pp.
Ishkov V.N., 1998, Izv. RAN, 62, 9, 835
Schrijver C., 2016, ApJ 820, Id, 103
Harra L.K., Schrijver C.J., Janvier M. et al., 2016, Sol. Phys. 291, 1761
Toriumi S., Schrijver C.J., Harra L.K. et al., 2017, ApJ 834, Id, 56
Hou Y.J., Zhang J., Li T. et al., 2018, arXiv:1808.06795 [astro-ph.SR]
Sun X. & Norton A.A., 2017, arXiv:1711.08383 [astro-ph.SR]
Yan X.L., Wang J.C., Pan G.M. et al., 2018, arXiv:1801.02290 [astro-ph.SR]
Wang H., Yurchyshyn V., Liu C. et al., 2018, arXiv:1801.02928 [astro-ph.SR]